

Figure S1

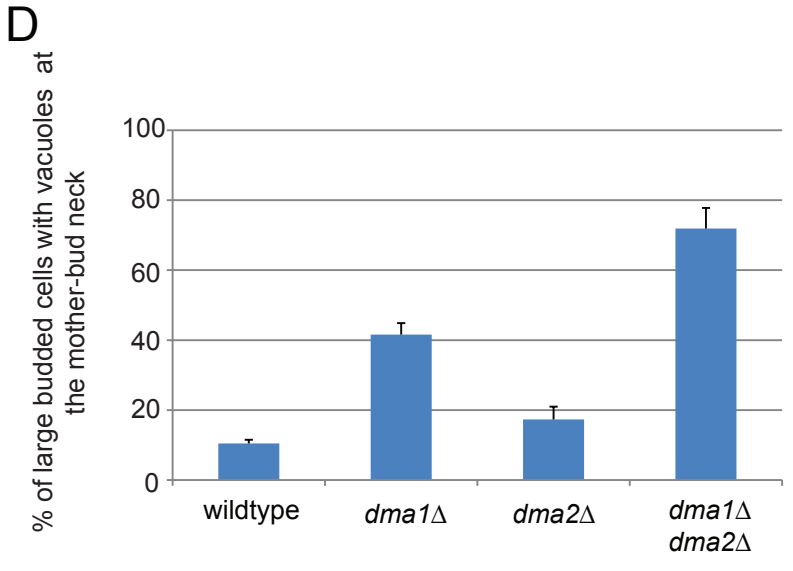
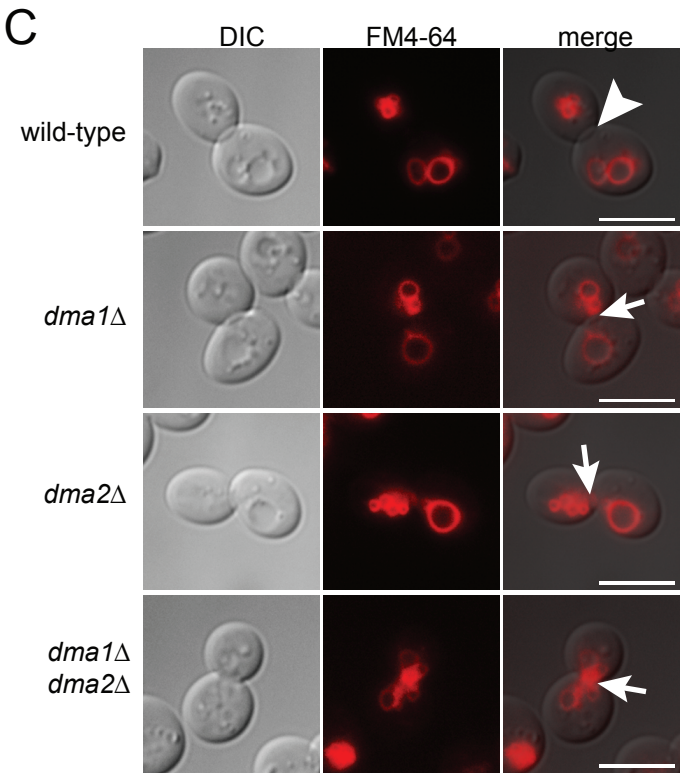
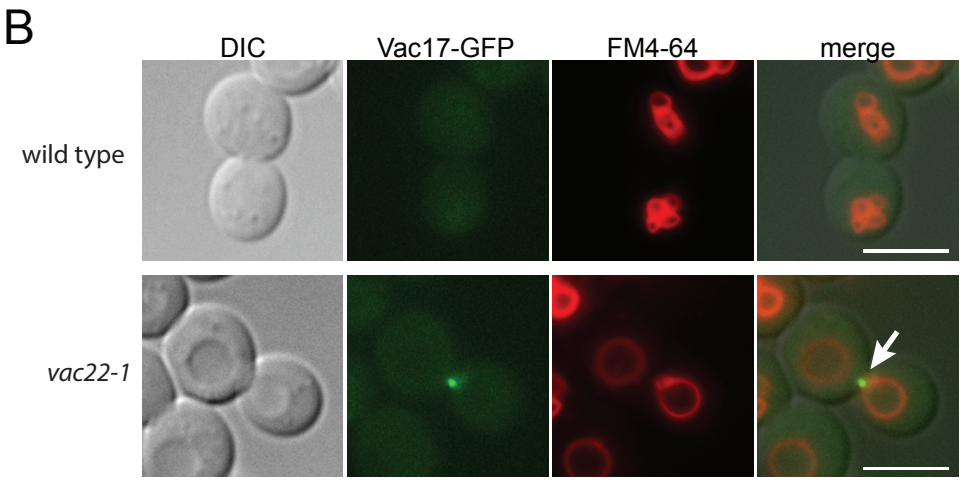
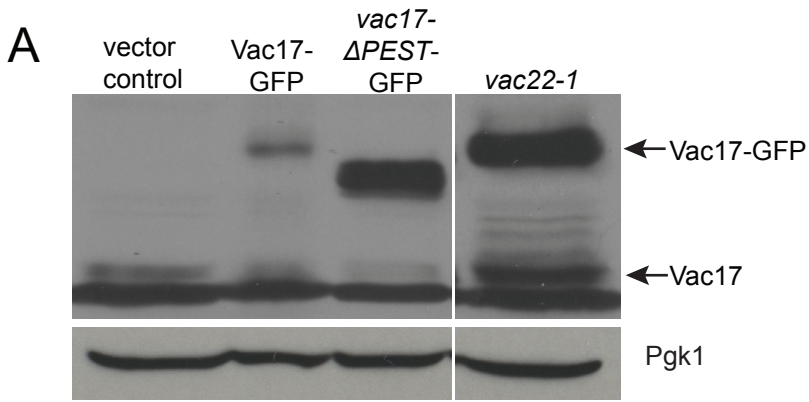


Figure S2

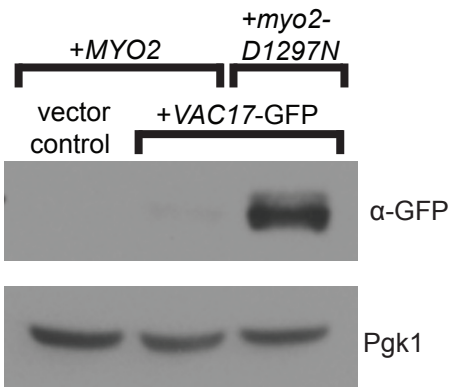


Figure S3

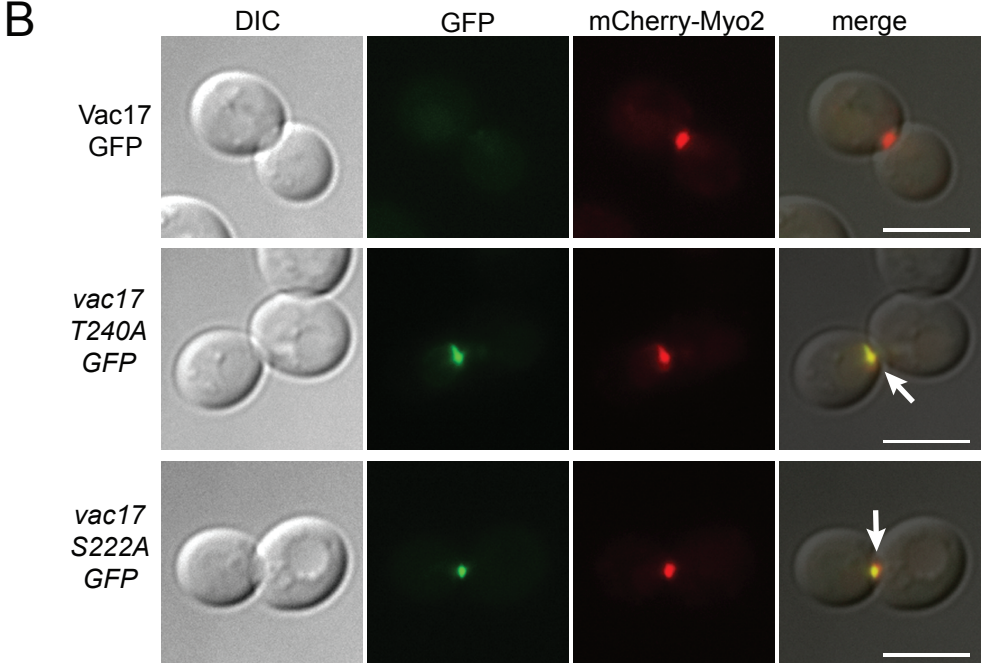
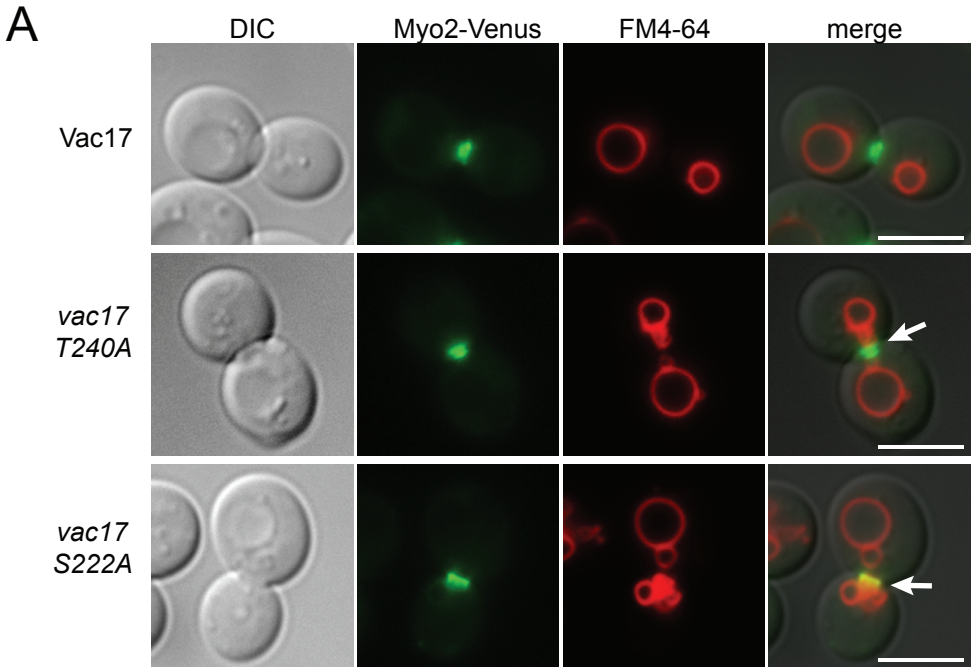


Figure S4

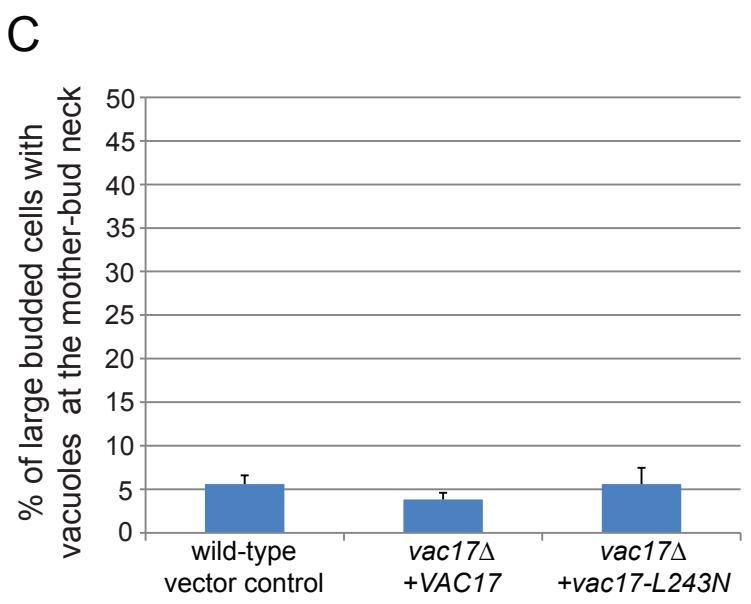
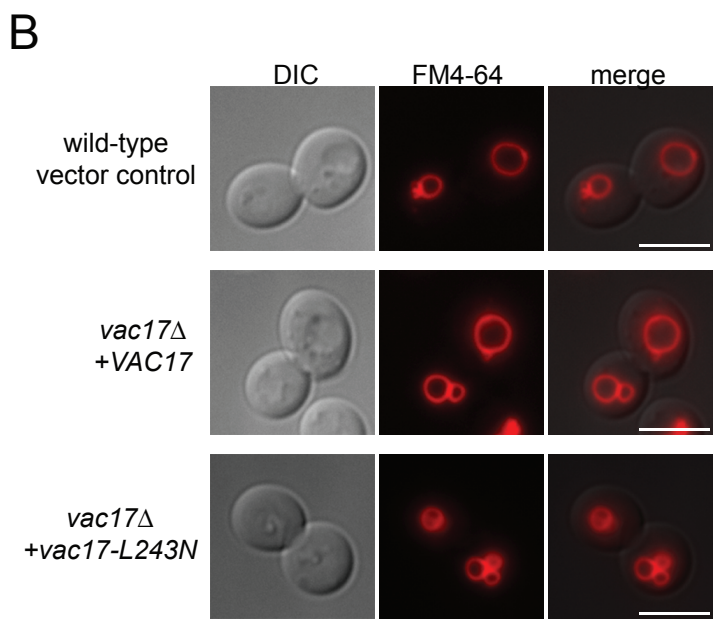
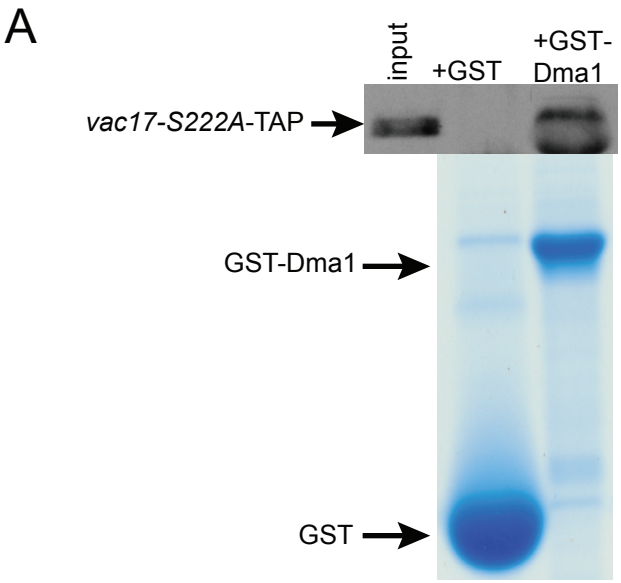
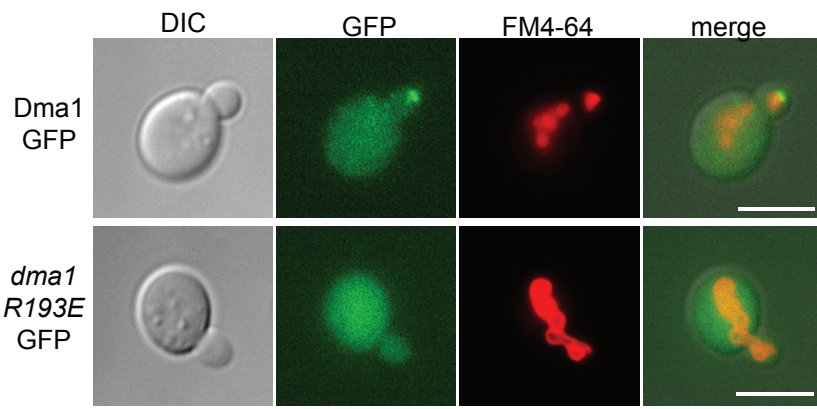


Figure S5

A



B

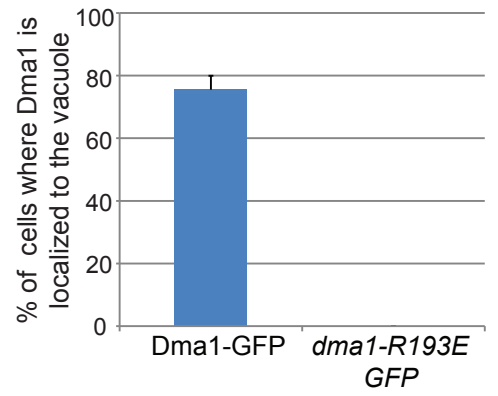
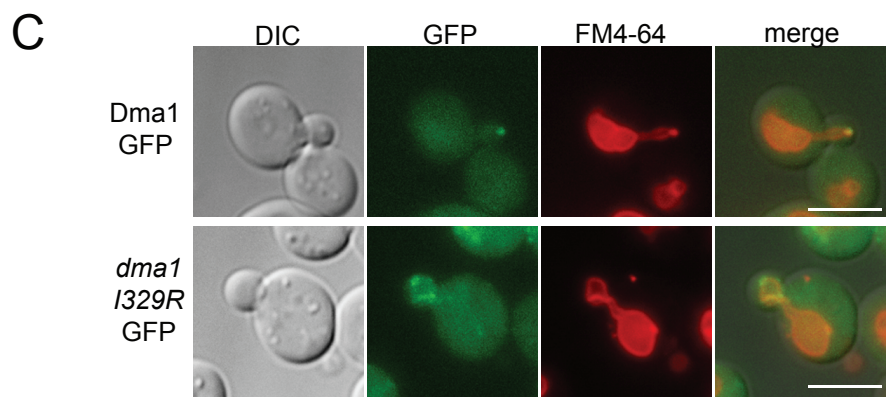
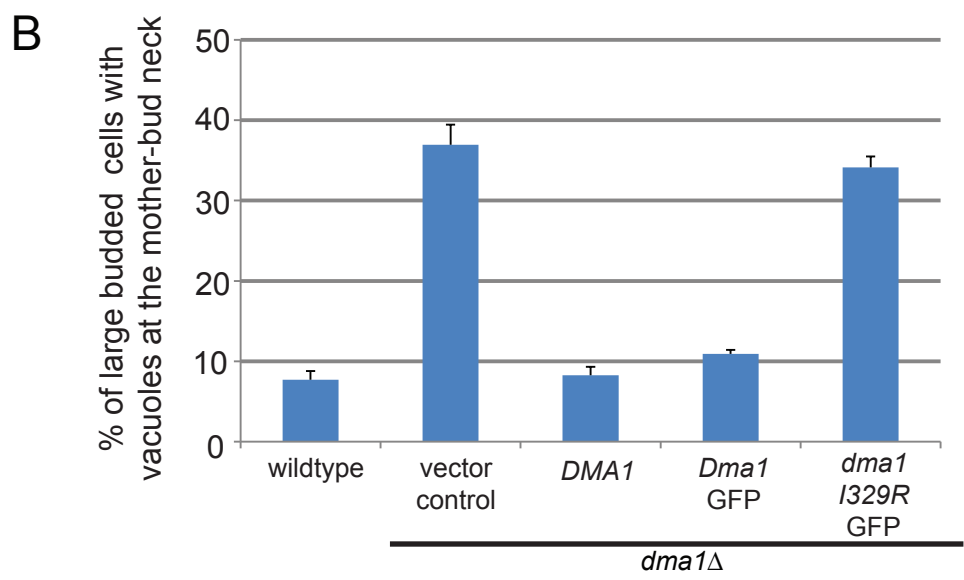
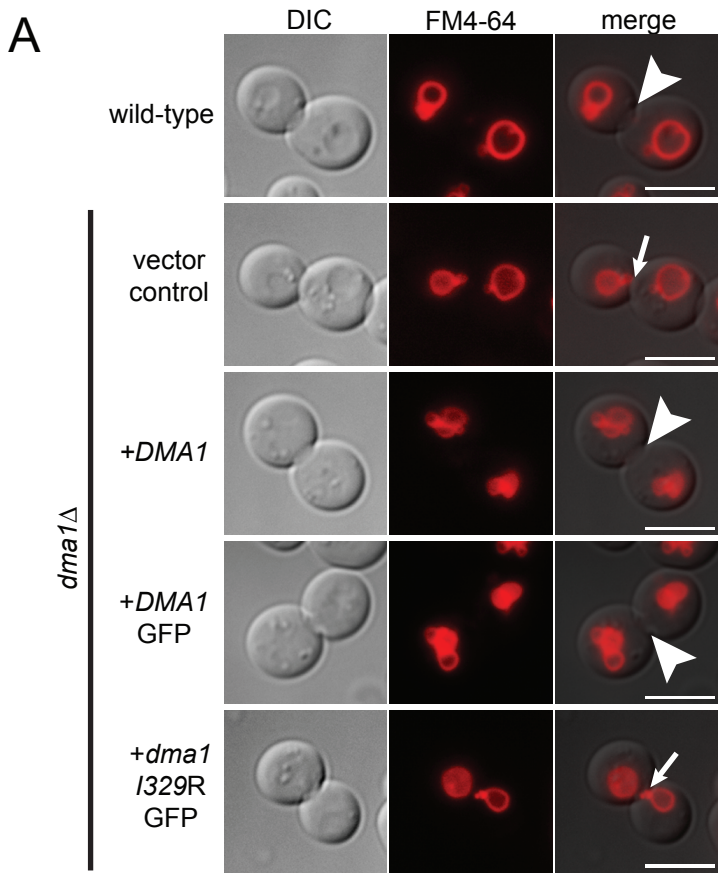


Figure S6



Supplemental Figure Legends

Figure S1, related to Figure 1. *DMA1* and *DMA2* are required for the detachment of the vacuole from Myo2. (A) The *vac22-1* mutant has elevated levels of both Vac17-GFP and endogenous Vac17. (B) Vac17-GFP and the vacuole are inappropriately transported to the mother-bud neck in the *vac22-1* mutant (arrow). (C) In the *dma1Δ*, *dma2Δ* and double *dma1Δ dma2Δ* mutants, termination of vacuole transport is defective (arrows). (D) Percentage of large budded cells with vacuoles accumulated at the mother-bud neck in the mutants shown in (C). anti-Vac17 antibodies; 1:1,000 dilution. anti-Pgk1 antibodies; 1:5,000 dilution. Error bars; SEM. Bar = 5 μm.

Figure S2, related to Figure 2. Vac17 levels are elevated when vacuole transport is blocked. A *myo2Δ vac17Δ* mutant expressing either *MYO2* or *myo2-D1297N* with *VAC17*-GFP from plasmids. Expression of *myo2-D1297N*, a mutant which is defective in binding Vac17 and vacuole transport, Vac17-GFP levels are elevated compared to cells expressing *MYO2*. anti-GFP antibodies; 1:1,000 dilution. anti-Pgk1 antibodies; 1:5,000 dilution.

Figure S3, related to Figure 3. *vac17* point mutants fail to dissociate from Myo2. (A) In cells expressing *vac17-T240A* and *vac17-S222A*, but not *VAC17*, vacuoles colocalize with Myo2-Venus at the mother-bud neck in large budded cells (arrows). (B) *vac17-T240A*-GFP and *vac17-S222A*-GFP, but not Vac17-GFP, colocalize with mCherry-Myo2 at the mother-bud neck (arrows) in large budded cells. Bar = 5 μm.

Figure S4, related to Figure 4. Characterization of Vac17 residues required for Dma1 to bind Vac17 and for the termination of vacuole transport. (A) GST-Dma1, but not the GST tag alone, binds *vac17-S222A-TAP* in yeast lysates. (B) The termination of vacuole transport occurs normally in the *vac17-L243N* mutant. (C) Quantification of the percentage of large budded cells with vacuoles at the mother-bud neck in wild-type cells and the *vac17Δ* mutant expressing either *VAC17* or *vac17-L243N*. A minimum of 100 cells were counted per experiment for 3 experiments. Error bars; SEM. Bar = 5 μm.

Figure S5, related to Figure 5. The FHA domain of Dma1 is required for the recruitment of Dma1 to the vacuole. (A) The *dma1-R193E-GFP* mutant fails to localize to the bud vacuole. (F) Quantification of the percentage of small budded cells where Dma1-GFP or *dma1-R193E-GFP* localizes to the vacuole. A minimum of 20 cells were counted per experiment for 3 experiments. Z-sections of small budded cells were analyzed. Error bars; SEM. Bar = 5 μm.

Figure S6, related to Figure 6. The E3 ubiquitin ligase activity of Dma1 is required for the termination of vacuole movement. (A) Expression of *DMA1* and *DMA1-GFP* but not an enzymatically inactive mutant, *dma1-I329R-GFP*, or vector control rescues the termination of vacuole movement in the *dma1Δ* mutant. Arrowheads; vacuoles are deposited properly in the bud and do not accumulate at the mother-bud neck. Arrows; vacuoles are mis-targeted to the mother-bud neck. (B) Percentage of large budded cells with vacuoles accumulated at the mother-bud neck in the *dma1Δ* mutant expressing vector control, *DMA1*, *DMA1-GFP* or *dma1-I329R-GFP*. A minimum of 100 cells were

counted per experiment for 3 experiments. Error bars; SEM. (C) *dma1-I329R*-GFP localizes to a broader area on the bud vacuole. Bar = 5 μ m.

Table S1, related to Experimental Procedures. Strains used in this study.

Table S2, related to Experimental Procedures. Plasmids used in this study.

Table S1, related to Experimental Procedures. Yeast Strains Used in this Study.

Strain	Genotype	Source
LWY7235	<i>MATa, ura3-52, leu2-3,-112, his3-Δ200, trp1-Δ901, lys2-801, suc2-Δ9</i>	Catlett and Weisman, 1998
LWY5798	<i>MATa, ura3-52, leu2-3,-112, his3-Δ200, trp1-Δ901, lys2-801, suc2-Δ9, vac17Δ::TRP1</i>	Tang et al., 2003
LWY7664	<i>MATa, ura3-52, leu2-3,-112, his3-Δ200, trp1-Δ901, lys2-801, suc2-Δ9, vac17Δ::TRP1, MYO2-GFP::HIS3</i>	Peng and Weisman, 2008
LWY12269	<i>MATa, ura3-52, leu2-3,-112, his3-Δ200, trp1-Δ901, lys2-801, suc2-Δ9, GFP-TUB1::URA3, kar9Δ ::kan^r, SPC42-mCherry::HIS3</i>	This study
LWY12086	<i>MATα, ura3-52, leu2-3,-112, his3-Δ200, trp1-Δ901, lys2-801, suc2-Δ9, vac17Δ::TRP1, myo2Δ::TRP1 [pRS413-mCherry-MYO2]</i>	This study
LWY11102	<i>MATa, ura3-52, leu2-3,-112, his3-Δ200, trp1-Δ901, lys2-801, suc2-Δ9, dma1Δ::kan^r</i>	This study
LWY11125	<i>MATα, ura3-52, leu2-3,-112, his3-Δ200, trp1-Δ901, lys2-801, suc2-Δ9, dma2Δ::kan^r</i>	This study
LWY11156	<i>MATa, ura3-52, leu2-3,-112, his3-Δ200, trp1-Δ901, lys2-801, suc2-Δ9, dma1Δ::kan^r, dma2Δ::kan^r</i>	This study
LWY11269	<i>MATα, ura3-52, leu2-3,-112, his3-Δ200, trp1-Δ901, lys2-801, suc2-Δ9, vac17Δ::TRP1, dma1Δ::kan^r</i>	This study
LWY11389	<i>MATa, ura3-52, leu2-3,-112, his3-Δ200, trp1-Δ901, lys2-801, suc2-Δ9, dma1Δ::kan^r, dma2Δ::kan^r, VAC17-TAP::LEU2</i>	This study
LWY11524	<i>MATα, ura3-52, leu2-3,-112, his3-Δ200, trp1-Δ901, lys2-801, suc2-Δ9, dma1Δ::kan^r, dma2Δ::kan^r, vac17-F225S-TAP::LEU2</i>	This study
LWY11528	<i>MATα, ura3-52, leu2-3,-112, his3-Δ200, trp1-Δ901, lys2-801, suc2-Δ9, dma1Δ::kan^r, dma2Δ::kan^r, vac17-L221P-TAP::LEU2</i>	This study
LWY11507	<i>MATα, ura3-52, leu2-3,-112, his3-Δ200, trp1-Δ901, lys2-801, suc2-Δ9, dma1Δ::kan^r, dma2Δ::kan^r, vac17-T240A-TAP::LEU2</i>	This study
LWY11541	<i>MATa, ura3-52, leu2-3,-112, his3-Δ200, trp1-Δ901, lys2-801, suc2-Δ9, dma1Δ::kan^r, dma2Δ::kan^r, vac17-S222A-TAP::LEU2</i>	This study
LWY11687	<i>MATα, ura3-52, leu2-3,-112, his3-Δ200, trp1-Δ901, lys2-801, suc2-Δ9, dma1Δ::kan^r, dma2Δ::kan^r, vac17Δ::TRP1</i>	This study
LWY8195	<i>MATa, ura3-52, leu2-3,-112, his3-Δ200, trp1-Δ901, lys2-801, suc2-Δ9, pep4-Δ1137, vac17Δ::TRP1, myo2Δ::TRP1 [YCp50-MYO2]</i>	This study
MHY501	<i>MATα, his3-Δ200, leu2-3, -112, ura3-52, lys2-801, trp1-1</i>	Chen and Hochstrasser, 1993

MHY1409	<i>MATα</i> , <i>his3-Δ200</i> , <i>leu2-3, -112</i> , <i>ura3-52</i> , <i>lys2-801</i> , <i>trp1-1</i> , <i>uba1-2</i>	Swanson and Hochstrasser, 2000
MHY605	<i>MATα</i> , <i>his3-11</i> , <i>leu2-3, -112</i> , <i>ura3-Δ5</i> , <i>pre1-1::can^R</i>	Chen and Hochstrasser, 1996
MHY952	<i>MATα</i> , <i>his3-Δ200</i> , <i>leu2-3, -112</i> , <i>ura3-52</i> , <i>lys2-801</i> , <i>trp1-1</i> , <i>doa3-delta1::HIS3 [YE_pDOA3_{LS}][YC_pUbDOA3ΔLS]</i>	Arendt and Hochstrasser, 1997
MHY973	<i>MATα</i> , <i>his3-Δ200</i> , <i>leu2-3, -112</i> , <i>ura3-52</i> , <i>lys2-801</i> , <i>trp1-1</i> , <i>doa3-delta1::HIS3 [YE_pDOA3_{LS}][YC_pUbDOA3ΔLS-T76A]</i>	Arendt and Hochstrasser, 1997
MHY1072	<i>MATα</i> , <i>his3-Δ200</i> , <i>leu2-3, -112</i> , <i>ura3-52</i> , <i>lys2-801</i> , <i>trp1-1</i> , <i>pup1::leu2::HIS3</i> , <i>pup3-delta2::HIS3 [Yc_{plac}22PUP1][Ye_{plac}181PUP3]</i>	Arendt and Hochstrasser, 1997
MHY1071	<i>MATα</i> , <i>his3-Δ200</i> , <i>leu2-3, -112</i> , <i>ura3-52</i> , <i>lys2-801</i> , <i>trp1-1</i> , <i>pup1::leu2::HIS3</i> , <i>pup3-delta2::HIS3 [Yc_{plac}22pup1-K58E][Ye_{plac}181pup3-E151K]</i>	Arendt and Hochstrasser, 2007

Table S2, related to Experimental Procedures. Plasmids Used in this Study.

Plasmid	Description	Source
pRS416- <i>DMA1</i>	CEN URA3	This study
pRS416- <i>dma1-G232R</i>	CEN URA3	This study
pRS416- <i>dma1-I329R</i>	CEN URA3	This study
pRS416- <i>dma1-I329-GFP</i>	CEN URA3	This study
pRS416- <i>DMA1-GFP</i>	CEN URA3	This study
pRS416- <i>DMA1</i> -tdTomato	CEN URA3	This study
pGEX4T-1 <i>DMA1</i>	Amp	This study
pGEX4T-1 <i>dma1-I329R</i>	Amp	This study
pRS413-mCherry- <i>MYO2</i>	CEN HIS3	Jin et al., 2011
pRS413- <i>MYO2</i> -Venus	CEN HIS3	This study
pRS415- <i>VAC17</i>	CEN LEU2	This study
pRS415- <i>VAC17-GFP</i>	CEN LEU2	This study
pRS416- <i>vac17-S222A</i>	CEN URA3	This study
pRS415- <i>vac17-S222A-GFP</i>	CEN LEU2	This study
pRS415- <i>vac17-T240A</i>	CEN LEU2	This study
pRS415- <i>vac17-T240A-GFP</i>	CEN LEU2	This study
pGEX4T-1 Myo2 cargo-binding domain	Amp	Pashkova et al., 2006
pRS416- <i>vac17-S202A</i>	CEN URA3	This study
pRS416- <i>vac17-S206A, S207A, S208A</i>	CEN URA3	This study
pRS416- <i>vac17-S213A</i>	CEN URA3	This study
pRS416- <i>vac17-T224A</i>	CEN, URA3	This study
pRS416- <i>vac17-S236A</i>	CEN URA3	Stringer and Piper, 2012
pRS416- <i>vac17-S247A, T248A</i>	CEN, URA3	This study
pVT102- <i>VAC17-GFP</i>	2 μ URA3	This study
pVT102- <i>VAC17</i>	2 μ URA3	Eves et al., 2012

Supplemental Experimental Procedures

***In Vitro* Binding and Competition Experiments**

Expression of GST tagged fusion proteins from BL21 star DE3 cells was induced with 0.4 mM IPTG (Denville Scientific); 16 °C overnight. Cells were resuspended in 50 mM Tris-HCl pH 7.5, 1 mM EDTA, 4 mM MgCl₂, 10% glycerol, 1 M NaCl, 5 mM DTT, 1 mM Pefabloc and Complete EDTA-free protease inhibitor cocktail (Roche) and lysed via sonication. An equal amount of lysis buffer without NaCl was added to the clarified lysates and incubated with glutathione Sepharose beads (GE Healthcare). Immobilized GST fusion proteins were washed with wash buffer (50 mM Tris-HCl pH 7.5, 4 mM MgCl₂, 10% glycerol, 0.5 M NaCl and 1 mM DTT and then with 50 mM HEPES-KOH pH 7.6, 150 mM KCl, 1 mM EDTA, 1 mM Na₃VO₄ and 10% glycerol). Yeast cells grown in YEPD at 24°C were resuspended in 50 mM HEPES-KOH, pH 7.6, 150 mM KCl, 1 mM EDTA, 20 mM sodium pyrophosphate, 10 mM NaN₃, 20 mM NaF, 1 mM Na₃VO₄, 100 mM β-glycerophosphate, 0.5% OG, 10% glycerol, 1X Protease inhibitor cocktail (Sigma) and Complete EDTA-free protease inhibitor cocktail (Roche) and lysed with glass beads. GST and GST fusion protein bound beads were incubated with clarified yeast cell extracts for 1 hour at 4 °C with agitation. Beads were then washed with wash buffer. Bound proteins were analyzed via SDS-page, Gelcode Blue staining (Thermo Scientific) and by immunoblot.

For competition experiments, GST-Dma1 bound beads were first incubated with 0.5 mg peptides resuspended in 50 mM HEPES-KOH pH 7.6, 150 mM KCl, 1 mM EDTA and 10% glycerol prior to incubation with yeast cell extracts.

Immunoprecipitation Experiments

TCA precipitated proteins were pelleted and washed with acetone. The dried protein pellets were resuspended in 200 μ l urea cracking buffer (6 M urea, 1% SDS, 50 mM Tris-HCl pH 7.5) and heated at 75 $^{\circ}$ C for 10 min. 1.8 ml TWIP buffer (50 mM Tris-HCl pH 7.5, 150 mM NaCl, 0.5% Tween-20, 0.1 mM EDTA) containing 1 mM Na_3VO_4 and 1X protease inhibitor cocktail (Sigma) was added to the resuspended protein.

Undissolved proteins were pelleted via centrifugation. 4 μ g of mouse anti-GFP antibodies (Roche) was added to the supernatant and incubated with agitation at 4 $^{\circ}$ C, overnight. 50 μ l of protein G beads (Sigma) washed with TWIP buffer was added and incubated with agitation at 4 $^{\circ}$ C for 1 hour. Beads were collected via centrifugation and washed with TWIP buffer. Bound proteins were analyzed via immunoblot.

For dephosphorylation of Vac17-GFP, Protein G beads were collected via centrifugation and washed 3 times with TWIP buffer without EDTA. The beads were resuspended in 1X λ -ppase buffer containing 1X protease inhibitor cocktail (Sigma) and 10 mM MnCl_2 . Either water, λ -ppase (400 units, New England Biolabs) or λ -ppase plus phosphatase inhibitors (100 mM NaF, 10 mM Na_3VO_4 , 50 mM EDTA, 20 mM β -glycerophosphate and 20 mM sodium pyrophosphate) were added to the samples. Phosphatase reactions were performed in a volume of 100 μ l and incubated at 30 $^{\circ}$ C for 1 hour. Reactions were terminated by addition of 50 μ l 2X SDS sample buffer and heated at 75 $^{\circ}$ C for 10 min.

Thermostability Measurements

Expression of GST tagged fusion proteins from BL21 star DE3 cells was induced with 0.1 mM IPTG (Denville Scientific); 16 $^{\circ}$ C overnight. Cells were harvested and

resuspended in 50 mM Tris-HCl pH 7.5, 150 mM NaCl, 0.1% Triton X-100, 5 mM β -mercaptoethanol, 1 mM Pefabloc and Complete EDTA-free protease inhibitor cocktail (Roche) and lysed via sonication. Triton X-100 was added to a final concentration of 1%. Clarified lysates were incubated with glutathione Sepharose beads (GE Healthcare) and washed with lysis buffer containing 0.01% Triton X-100. Bound proteins were eluted in wash buffer containing 25 mM glutathione and 50 mM NaOH. Recombinant proteins were then purified on a size exclusion column (HiLoad 16/60 Superdex 200; GE Healthcare). Protein unfolding was measured using a ThermoFluor plate reader (Johnson and Johnson). Samples containing ~0.2 mg/ml protein, 1 mM peptide and 100 μ M 8-Anilino-1-naphthalenesulfonic acid (ANS, Sigma) were prepared in a 384-well plate and fluorescence was measured from 15 $^{\circ}$ C to 80 $^{\circ}$ C in 1 $^{\circ}$ C increments. Melting temperatures were determined automatically using the ThermoFluor Acquire software.

Supplemental References

Arendt C.S., and Hochstrasser M. (1997). Identification of the yeast 20S proteasome catalytic centers and subunit interactions required for active-site formation. *Proc Natl Acad Sci U S A.* 94:7156-61.

Catlett N.L., and Weisman L.S. (1998). The terminal tail region of a yeast myosin-V mediates its attachment to vacuole membranes and sites of polarized growth. *Proc Natl Acad Sci U S A.* 95:14799-804.

Chen P., and Hochstrasser M. (1996). Autocatalytic subunit processing couples active site formation in the 20S proteasome to completion of assembly. *Cell.* 86:961-72.

Chen P., Johnson P., Sommer T., Jentsch S., and Hochstrasser M. (1993). Multiple ubiquitin-conjugating enzymes participate in the in vivo degradation of the yeast MAT alpha 2 repressor. *Cell.* 74:357-69.

Eves, P.T., Jin, Y., Brunner, M., and Weisman, L.S. (2012). Overlap of cargo binding sites on myosin V coordinates the inheritance of diverse cargoes. *The Journal of cell biology* 198, 69-85.

Jin, Y., Sultana, A., Gandhi, P., Franklin, E., Hamamoto, S., Khan, A.R., Munson, M., Schekman, R., and Weisman, L.S. (2011). Myosin V transports secretory vesicles via a Rab GTPase cascade and interaction with the exocyst complex. *Developmental cell* 21, 1156-1170.

Pashkova N., Jin Y., Ramaswamy S., and Weisman L.S. (2006). Structural basis for myosin V discrimination between distinct cargoes. *EMBO J.* 25:693-700.

Peng Y., and Weisman L.S. (2006). The cyclin-dependent kinase Cdk1 directly regulates vacuole inheritance. *Dev Cell.* 15:478-85.

Stringer D.K., and Piper R.C. (2011). A single ubiquitin is sufficient for cargo protein entry into MVBs in the absence of ESCRT ubiquitination. *J Cell Biol.* 192(2):229-42.

Swanson R., and Hochstrasser M. (2000). A viable ubiquitin-activating enzyme mutant for evaluating ubiquitin system function in *Saccharomyces cerevisiae*. *FEBS Lett.* 477:193-8.

Tang F., Kauffman E.J., Novak J.L., Nau J.J., Catlett N.L., and Weisman L.S. (2003). Regulated degradation of a class V myosin receptor directs movement of the yeast vacuole. *Nature.* 422:87-92.

Tang F., Peng Y., Nau J.J., Kauffman E.J., and Weisman L.S. (2006). Vac8p, an armadillo repeat protein, coordinates vacuole inheritance with multiple vacuolar processes. *Traffic.* 7:1368-77.